We are IntechOpen, the world's leading publisher of Open Access books Built by scientists, for scientists

6,100
Open access books available

167,000
International authors and editors

185M
Downloads

Our authors are among the

154
Countries delivered to

TOP 1%
most cited scientists

12.2%
Contributors from top 500 universities

CLARIVATE ANALYTICS

BOOK CITATION INDEX

INDEXED

WEB OF SCIENCE™

Selection of our books indexed in the Book Citation Index
in Web of Science™ Core Collection (BKCI)

Interested in publishing with us?
Contact book.department@intechopen.com

Numbers displayed above are based on latest data collected.
For more information visit www.intechopen.com

Chapter

Cyclo-Stationarity in Sea Level Variability from Satellite Altimetry Data and Correlation with Climate Indices in the Mediterranean Sea

Dimitrios A. Natsiopoulos, Eleni A. Tzanou and Georgios S. Vergos

Abstract

The exploitation of altimetric datasets from past and current satellite missions is crucial to both oceanographic and geodetic applications. For oceanographic studies, they allow the determination of sea level anomalies as deviations from a static mean sea level. This chapter deals with numerical experiments for the statistical analysis of Sea Level Anomaly (SLA) variations in the Mediterranean. SLA empirical covariance functions were calculated to represent the statistical characteristics of the sea variation for the period between 2002 and 2016. The variation of monthly SLA time series was investigated, and a correlation analysis was performed in terms of epoch-based pattern re-occurrence. To identify possible correlations with global and regional climatic phenomena that influence the ocean state, three indexes have been investigated, namely the Southern Oscillation Index (SOI), the Mediterranean Oscillation Index (NOI), and the North Atlantic Oscillation (NAO). Finally, Empirical Orthogonal Functions (EOF) and Principal Component Analysis (PCA) were applied to all SLA time series and for each satellite mission to extract the individual dominant modes of the data variability. After the analysis, the SLA field is separated into spatial structures (EOF modes) and their corresponding amplitudes in time, the Principle Components (PCs).

Keywords: SLA, EOF, variance, MOI, NAO, SOI, variability, cyclo-stationarity

1. Introduction

Fluctuations in the sea level is a significant problem, as the sea level continues to rise dramatically [1, 2]. Regarding Europe, sea level rise is very important, as especially in the Mediterranean Sea, the majority of the population is concentrated along the coastline [3–6]. Almost 529 million citizens live around Mediterranean countries, with 205 million (~39%) on the northern shore and 324 million on the southern and eastern shores. According to existing demographic projections, this number can reach as high as 611 million within next three decades. By 2025, one-third

of the Mediterranean population will live on the northern shore and two-thirds on the southern and eastern shores [7].

The population growth rate in coastal areas is accelerating, and increasing tourism adds to the pressure on the environment mainly by increasing the vulnerability of coastal ecosystems. Countryside and residences are changed, affected and destroyed by either direct human intervention or as a byproduct of the increasing anthropogenic activity in coastal areas. As sea level rises, increased salinity in groundwater could affect access to drinking water and agricultural inputs. Flooding and the destruction of infrastructure in food-producing areas is a likely result of sea level rise. Coastal erosion with environmental, social and economic impact will result in repercussions that will affect large coastal population. Tourism industry with all its activities (hotels, transports etc), a sector that several economies depend on can be lost forever [8–17].

The global sea level level is rising extremely fast. Several studies during the last twenty years have shown that new records of sea level are set with the projections for the future to be even more discouraging. As a result, sea level variations with time and their projections are of high importance. Global tides-gauge data over the last century showed a rise of 18.5 cm [18], while similar studies using only tide-gauge data from coastal areas have been done for the Mediterranean [15, 19–21]. On the other hand, studies using annually averaged satellite altimetry data from various missions show a somewhat higher rate (3 to 7 mm) of rising than tide gauge (TG) data [22–25].

Fluctuations in water temperature, salt content and added water volume especially from melting glaciers contribute to the short and long-term variations. The significant positive trend in sea level rise rely mainly on global Earth's temperature increase and on thermal expansion of Earth itself [26]. Therefore, observing the fluctuations of sea level along with the trends is crucial as it can be a decisive factor in coastal areas tracking system for their decisive management.

Satellite altimetry offer high accuracy and resolution information for sea surface heights for almost the last half century, increasing the in-situ sea level measurements from tide-gauge found both on offshore and coastal areas. Altimetry focused satellites, with the low resolution mode (LRM) data from the first missions to the last synthetic aperture radar (SAR) observations from Cryosat-2 and Sentinel satellites increased the surface observations, resulting in a constant global coverage of sea. The concept of this technique is based on the transmission of the altimeter sensor, located on the bottom part of the satellite, of a microwave or laser pulse to the sea surface and its reflection of water. The distance between the satellite and the sea-surface is given by the distance formula, by multiplying the speed of light by the two-way travel time (see **Figure 1**). Taking into account the satellite altitude from a surface (ellipsoid), Sea Surface Heights (SSH) are available for time of the measurement. This is the main advantage of satellite altimetry, as it provides real time and precise information over seas. Moreover, the short, repeated period of the latest altimetry missions tend to be a very useful tool for the estimation of the sea level rise as increases the temporal sampling rate of sea surface heights measurements.

Many studies have been conducted in the past concerning the calculation of mean sea surface (MSS) models from altimetry data with of these studies presenting global models [27, 28] or regional ones [29–32]. Compared to other older techniques like tide gauge or shipborne data collection, satellite altimetry can provide high-resolution and precision information both for ocean and geophysics and several studies including gravity, dynamic ocean topography, circulation, temperature etc. rely on altimeter data [33–35].
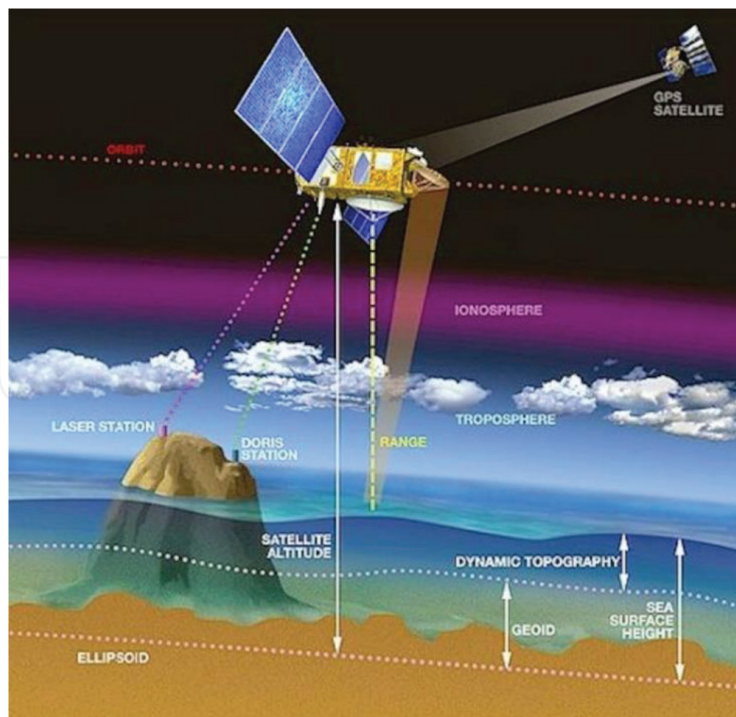
Figure 1.
Principle of satellite altimetry (credit AVISO, 2021).

Based on the previously mentioned, this study aims to analyze the available Envisat, Jason-1, Jason-2 and Cryosat-2 data in the form of Sea Level Anomalies (SLAs) spanning the Mediterranean Sea. Although Mediterranean basin is nearly enclosed by land, mainly on the north (Europe) and on the south (Africa), variations of sea level can be analyzed as the altimetry data cover a very long period of repeated measurement ground footprints. By studying the empirical covariance functions computed for all altimetry missions available for this study, spanning the years from 2002 to 2016, variations of SLAs can be further analyzed and useful conclusions on sea level variation can be defined. Based on this, results confirming the cyclo-stationarity of the SLAs can be inferred and connected with climate change indices over the oceans. To this extent, three such indexes have been investigated, namely the Southern Oscillation Index (SOI), the Mediterranean Oscillation Index (NOI), and the North Atlantic Oscillation (NAO). Finally, the last step in this study, involves the Principal Component Analysis (PCA). PCA employed the data of each satellite mission separately or the whole data as well. Through this method, dominant patterns can be extracted, identifying thus either annual or seasonal modes, signal or noise.

## 2. Area under study, available data and pre-processing

As already mentioned, the area under study covers the whole Mediterranean Sea, from Europe to Africa on the north–south direction and from strait of Gibraltar to Levant on the West -East direction with four altimetry missions studied in this work, Envisat, Jason-1, Jason-2, and Cryosat-2. For Jason-1, data from the various phases of the mission have been used. These comprise of data from phase A, from 15/1/2002 (cycle 1) to 26/1/2009 (cycle 259) resulting in a total number of 689,680 observations; data from phase B, during the period from 10/2/2009 (cycle 262) to 3/3/2012

(cycle 374) (512,996 observations) and from the geodetic phase (phase C), during the period from 7/5/2012 (cycle 382) to 21/6/2021 (cycle 425) and a total number of 120,973 observations (see **Figure 2** for the Jason –1 data distribution).

During phase A, each Jason-1 cycle consists of 254 passes, with almost 20% of those having available observations in the Mediterranean Sea within the satellite's period of 10 days. In phase B, the new orbit was adjacent to that of Jason-2 and covered the oceans every 4.5 days while in phase C, the satellite was set in a drifting orbit to perform a geodetic, i.e., higher resolution, mapping. For Envisat satellite, 881,657 point values (see **Figure 3**) compose phase A, within the period 14/5/2002 and 22/10/2010 (cycle 6 to cycle 77) and 150,435 points phase B with cycles 95 to 113. The values mesh is much denser than Jason-1 and is consists of 1003 passes with four times less cross-track spacing at the equator (~75 to ~300 km).
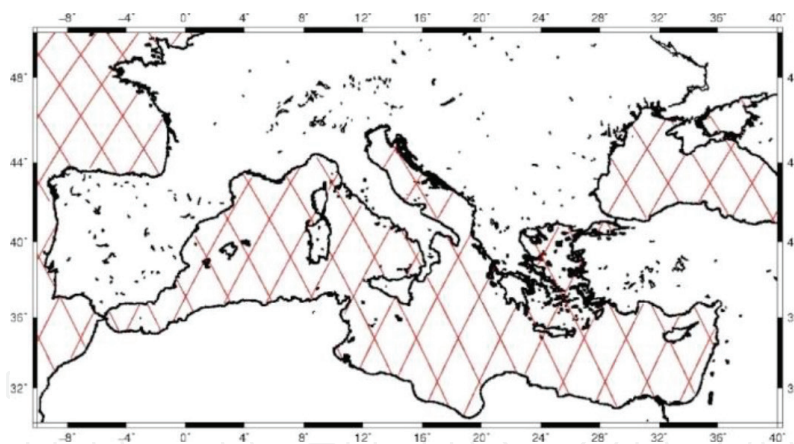
The orbit of Jason-2 was the same as that of the Jason-1 and Topex/Poseidon satellites. Data collection started with cycle 0 on 4/7/2008, and phase A ended on 2/10/2016 with cycle 303. This 8 year period of data collection resulted in 1,061,379
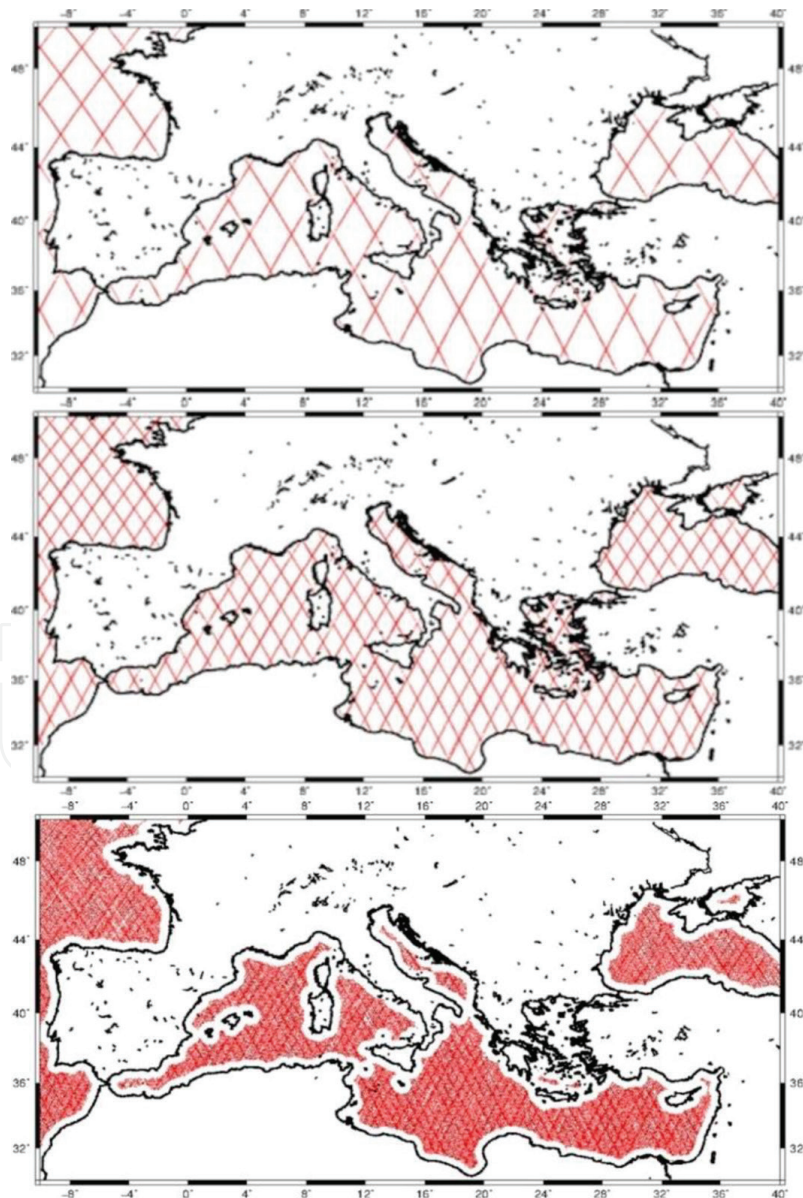
Figure 2.
*Jason-1 data distribution. Phase A (up), B (middle) C (bottom).*
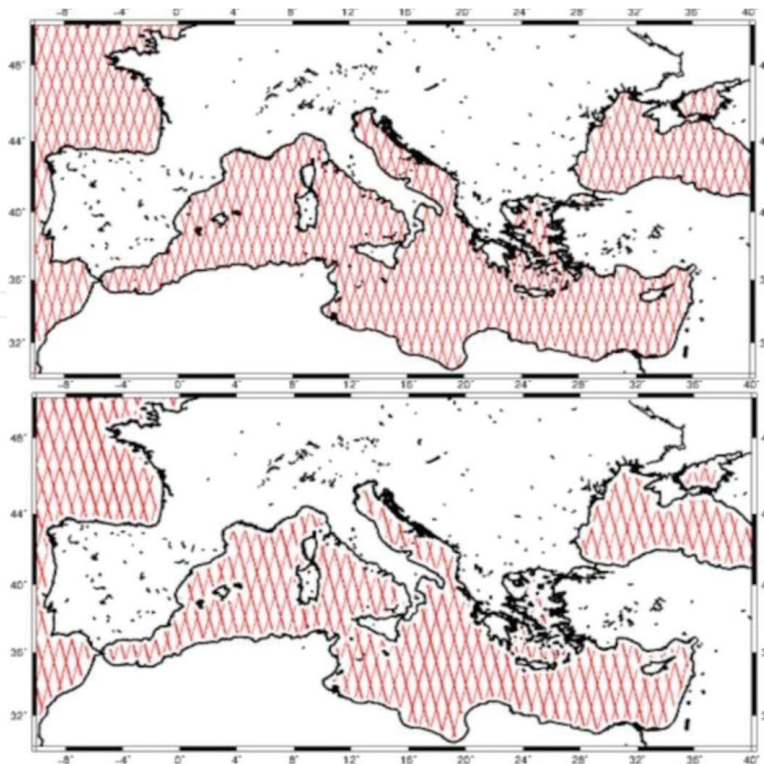
Figure 3.
Envisat data distribution. Phase A (up), B (bottom).

Figure 4.
Jason-2 data distribution.

point values in the Mediterranean Sea (**Figure 4**). Then the second phase of the satellite mission started with a new orbit until May 2017. This second phase of the mission is not included in our study.

The last mission used in this study, is that of the Cryosat-2 altimetry satellite. Cryosat-2 is the successor of Cryosat-1, whose mission was canceled after the failed launch on 2005. Its successor was launched in April 8, 2010 and the data collection started with cycle 4 on July 14 of the same year. Until cycle 73, the satellite records referred to low-resolution (LRM) and synthetic aperture radar (SAR) data, which where then succeeded by SAR and SAR interferometric (SARin) data getting closer to the coastline. Until the end of 2016 78 months of data have been collected with 826,941 point values being available (**Figure 5**).
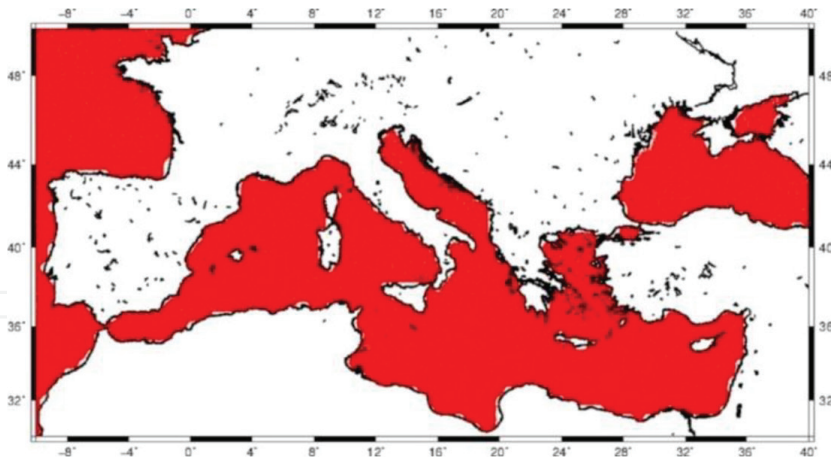
Figure 5.
Cryosat-2 data distribution.

The data for this study were obtained through the Radar Altimeter Database System (RADS) operated by the Delft Institute for Earth-Oriented Space research (DEOS) was used (RADS 2011). RADS provides a platform with a large variety of altimetry missions. This database was chosen as the platform provides not only the geophysical data records, with all the necessary corrections for the altimeter data, but has the additional benefit that all records refer to the same ellipsoid ensuring that there are no reference system problems in the form of biases when combining data from multiple satellite missions [31, 36]. Moreover, the RADS altimetry data are already processed through the method of crossover adjustment for the reduction of radial orbit errors, while it provides a one stop point to collect multi-satellite data instead of retrieving them from various sources.

The platform provides the user various options for the reference surface of SLAs, among which that of the EGM2008 geoid [37], was chosen along with be zero-tide (ZT) geoid model ensuring that the tidal system is the same with the one of the altimetric data. RADS provide also to the user the opportunity to choose along various geophysical corrections and models for the systematic errors that affect the altimeter data quality. In this work the following selections were made:

• ECMWF for the dry tropospheric correction

• MWR (NN) for the wet tropospheric correction

• the smoothed dual-frequency model for the ionospheric correction,

• GOT4.7 for the ocean and pole tide

• the CLS Sea State Bias (SSB) model for the SSB effect.

The Inverse Barometer (IB) correction which is also provided in the geophysical data records, in three different types, local, global and total, was applied to the raw data after the aforementioned geophysical corrections. **Tables 1–4** tabulates the statistics of the SLAs values before and after the application of total IB corrections total inverse barometer corrections. From these Tables, except for the minmax values which are obviously attributed to blunders and their locations are close to shore, it

	nr. values	min	max	mean	std
SLA	689,860	−1.817	0.880	0.007	±0.150
SLA + total IB	689,860	−1.694	0,894	0,059	±0.139

Table 1.
Statistics of JASON-1 phase a data with and without total IB correction. Unit: [m].

	nr. values	min	max	mean	std
SLA	512,995	−1.092	1.069	0.036	±0.160
SLA + total IB	512,995	−0.918	1.150	0.076	±0.148

Table 2.
Statistics of JASON-1 phase B data with and without total IB correction. Unit: [m].

	nr. values	min	max	mean	std
SLA	120,973	−0.749	0.799	0.051	±0.145
SLA + total IB	120,973	−1.136	0.842	0.086	±0.137

Table 3.
Statistics of JASON-1 phase C data with and without total IB correction. Unit: [m].

	nr. values	min	max	mean	std
SLA	881,612	−2.781	1.179	0.032	±0.146
SLA + total IB	881,612	−2.727	1.304	0.078	±0.176

Table 4.
Statistics of ENVISAT data with and without total IB correction. Unit: [m].

can be concluded that IB correction little affect the statistics as difference of few cm (~2–4) are noticed in mean and standard deviation values.

In order to remove the blunders noticed in the SLA data, a 3σ test was performed. The small mean values, close to a zero mean, is a good indication, that all altimetry data used in this work, as to being unbiased (0.7 cm (Jason-1 ph. A) to 5.1 cm (Jason-1 ph. C). The result of the 3σ test is that all SLA values larger than the one of 3σ, are extracted from the final data used. **Table 5** above tabulates the statistics of all SLAs after the 3σ removal test (see the top row of **Tables 1–4** and **6** for comparison). In case of Jason-1, only 26,581 (~2%) of the point values were extracted from three phases, resulting in a reduction of 70 cm. ~1.1% of ENVISAT point values we removed, resulting again in a significant discount at the range of data (~1.4 m). For Jason-2 data, 26,851 point values were removed (~2.8%), while for Cryosat-216,294

	nr. values	min	max	mean	std
SLA	944,941	−1.864	1.686	0.024	±0.156
SLA + total IB	944,941	−0.441	0.441	0.061	±0.134

Table 5.
Statistics of Cryosat-2 data with and without total IB correction. Unit: [m].

	nr. values	min	max	mean	std
SLA	1,061,379	−0.783	1.168	0.047	±0.153
SLA + total IB	1,061,379	−0.787	1.214	0.094	±0.141

Table 6.
Statistics of Jason-2 data with and without total IB correction. Unit: [m].

	nr. values	min	max	mean	std
Jason-1 ph. A	675,041	−0.416	0.416	0.050	±0.124
Jason-1 ph. B	504,763	−0.444	0.444	0.067	±0.141
Jason-1 ph. C	117,443	−0.351	0.351	0.073	±0.117
ENVISAT	871,584	−0.527	0.527	0.072	±0.147
Jason-2	1,031,247	−0.423	0.423	0.082	±0.123
Cryosat-2	928,647	−0.441	0.441	0.061	±0.134

Table 7.
Statistics of all SLAs after the 3σ. Unit: [m].

(~1.7%) of the data were identified as blunders. The reduction of the data range was similar to the other missions from ~2.2 m to 0.8 m (**Table 7**).

3. Sea level anomaly variations in the Mediterranean Sea and correlation with global and regional climatic phenomena

As already mentioned, the present study is focused on the entire Mediterranean basin, within the region bounded between $30° \leq \varphi \leq 50°$ and $−10° \leq \lambda \leq 40°$. In this region, the statistical characteristics of the SLA have been studied using altimetric observations from various satellites for the period 2002–2016. For each mission, the analysis presented here refers to monthly data as only data falling in the specific time period have been used. Each test refers to the use of the entire set of satellite passes for the Mediterranean Sea, so that the SLA variability will be studied in cross-track (2D) direction (see **Figures** 2-5). The computation of empirical covariance functions allowed the investigation of the statistical characteristics of the SLA. The equation of the empirical covariance function for a group of data, for our study (h^{SLA}), under a known spherical distance ψ is ([38]):

$$C\left(h_i^{SLA},,h_j^{SLA},,\psi\right) = M\left\{h_i^{SLA},h_j^{SLA}\right\}_{\psi} \qquad (1)$$

where, M denotes the mean value operator and i,j the SLA observations at two points in the area under study with a distance ψ. Employing Eq. 1, the empirical covariance functions have been estimated for all available satellite cycles. Given the monthly availability of data, it is implied that for each year 12 covariance functions have been determined. As a result, an analysis of the SLAs variances calculated through the covariances functions has been performed for the whole period that the satellite data cover in this study.

As already mentioned in the introduction of this work, sea level variations can also attributed to climate episodes. Thus, three climate indexes have been studied. Southern Oscillation Index (SOI) reflects the sea response to El Niño/La Niña-Southern Oscillation (ENSO) events indicating the evolution and the volume of the two events in the Pacific Ocean. Positive values may lead to La Niña event while on the contrary, negative values are probably a result of El Niño phenomena. For the computation of the value, differences of pressure between Tahiti and Darwin are taken into account [39–41].

The second index to be investigated was NAO, an index that provides information for climate variations in the North Atlantic Ocean. In the area of interest, positive values indicate dry winters while for the same season warmer and more wet conditions can be found in other part of Europe. On the other hand, negative values indicate humid atmosphere in the south part of Europe and frozen air in the north. For the computation of index values, surface sea-level pressure difference between the Subtropical High and the Subpolar Low are used [42–46]. The most proper index for studying the correlation between the sea level and climatic phenomena is MOI as it refers to pressure differences between Algiers and Cairo or Gibraltar and Israel. In both cases, positive values indicate dry conditions in the Mediterranean mainly in the north-west segment while negative values are connected with cyclones and wet conditions in the west [47–50]. For the present study, data for these indices have been acquired from the Climate Research Unit of the University of East Anglia (http://www.cru.uea.ac.uk/).

Figures 6-**9** below depict the SLA variances along with the SOI, NAO and MOI indices for all consecutive months within each year between 2002 and 2011 for Jason-1 satellite, 2008 and 2016 for Jason-2, 2002 and 2012 for ENVISAT satellite and 2010 and 2016 for Cryosat-2 satellite. Consecutive negative values of SOI lower than -0.7 indicate El Niño phenomena and positive values larger than 0.7 La NiñaFor all missions, it can be summarized that despite the delay of ~one semester, there is a connection between the El Niño and the La Niña events and SLA change in the Mediterranean. The smallest value of SOI in early 2005 resulted in large variance in the summer of 2005 both on Envisat (~320 cm^2) and Jason-1(~240 cm^2). Moreover, the evolution of El Niño in Spring of next year had a faster stamp on SLA variation as the values are rising during Summer and Autumn (from 170 cm^2 to 280 cm^2 for Envisat and from 100 cm^2 to 250 cm^2 for Jason-1) [51, 52]. Similar results are found while studying the severe La Niña episodes during the last months of 2007, the first and the last of 2008 and the start of 2009. Strong La Niña during 2010–2011 and El Niño during 2015–2016 resulted in significant variations in SLAs. For Jason-2, the variance from 324 cm^2 in April 2010 decreased to 98 cm^2 while after El Niño the variance from 102 cm^2 in September 2014 reached the 300 cm^2 in February 2015 [53, 54].

The geometry and the shape of the Mediterranean along with the location of ENSO events result that this index is not the most proper for studying the response of SLA to climatic phenomena. Once the NAO is examined, the heavier relation between SLA and pressure can be noticed. The increasing of the index results in fast falls of SLA variation. This is noticed mainly during winter while during summer the variation in sea level due to changes in NAO values are not so instant. Same results are found in similar study [48] which signals that atmospheric forcing is not the contributing factor to the steric sea level variations in the Mediterranean during the summer period. Positive values of the index in early 2007, 2008, and 2011 resulted in a decrease of the variance, from 286 cm^2 in December 2006 to 120 cm^2 in July 2007,
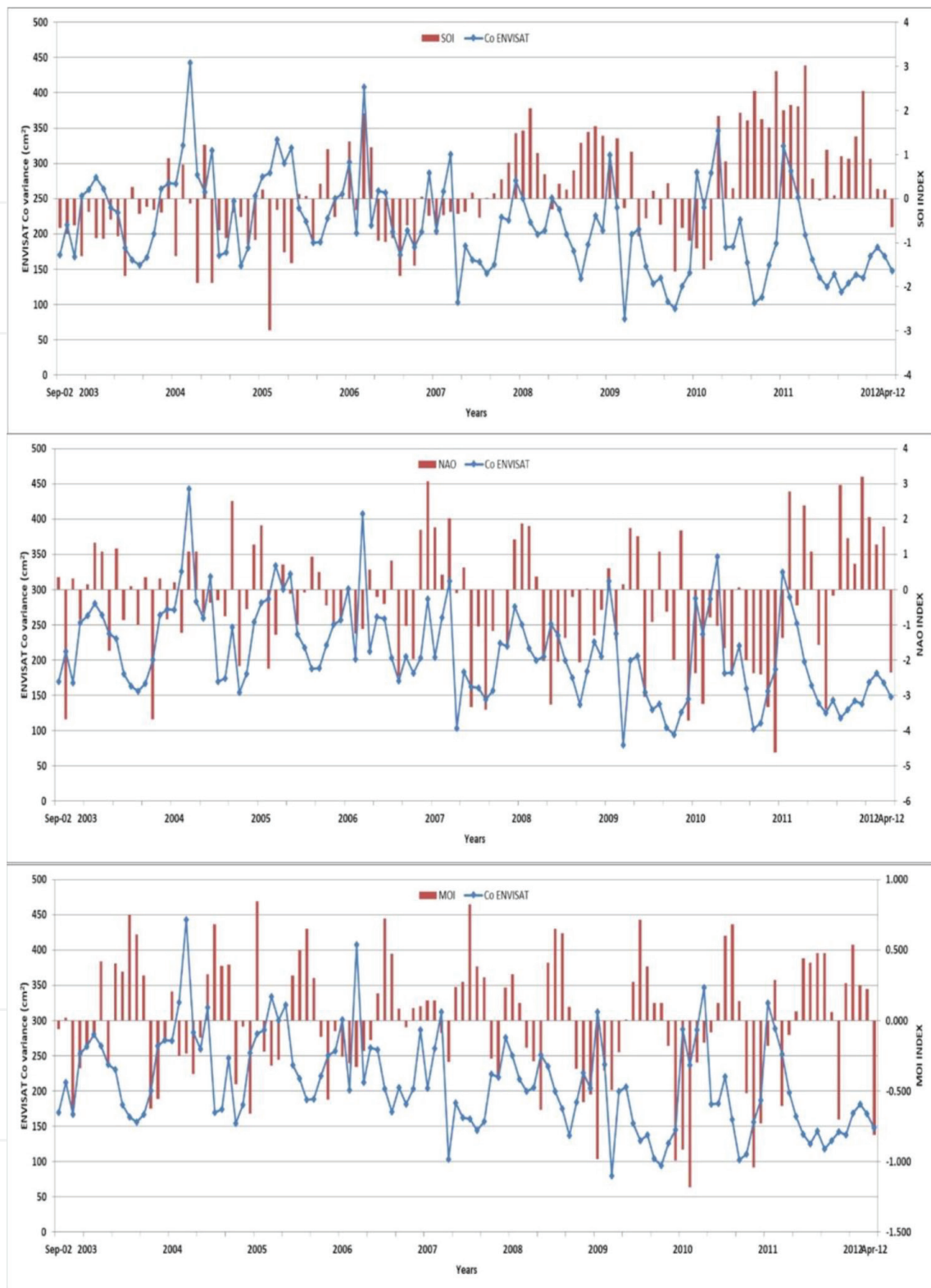
Figure 6.
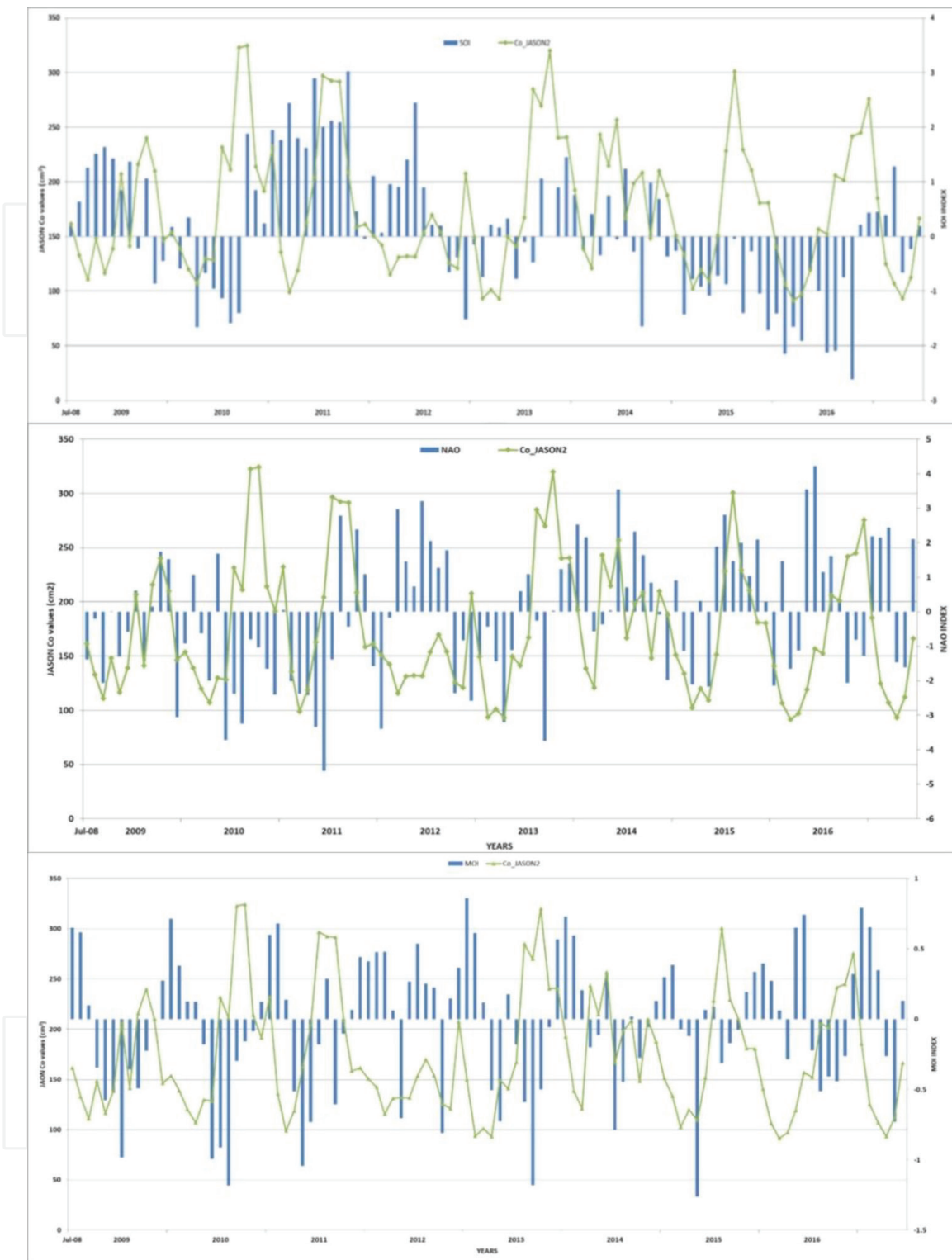*ENVISAT SLA variances fluctuations from 2002 to 2012 and correlation with SOI (up), NAO (middle) and MOI (bottom).*

and from 212 cm^2 in March 2008 to 93 cm^2 in July 2008 for Envisat, while negative values mainly in summer and autumn months increased the variance from 87 cm^2 in September 2002 to 252 cm^2 in February 2003 and from 130 cm^2 in September 2010 reached the 333 cm^2 in early 2011 for Jason-1 [42, 55, 56].
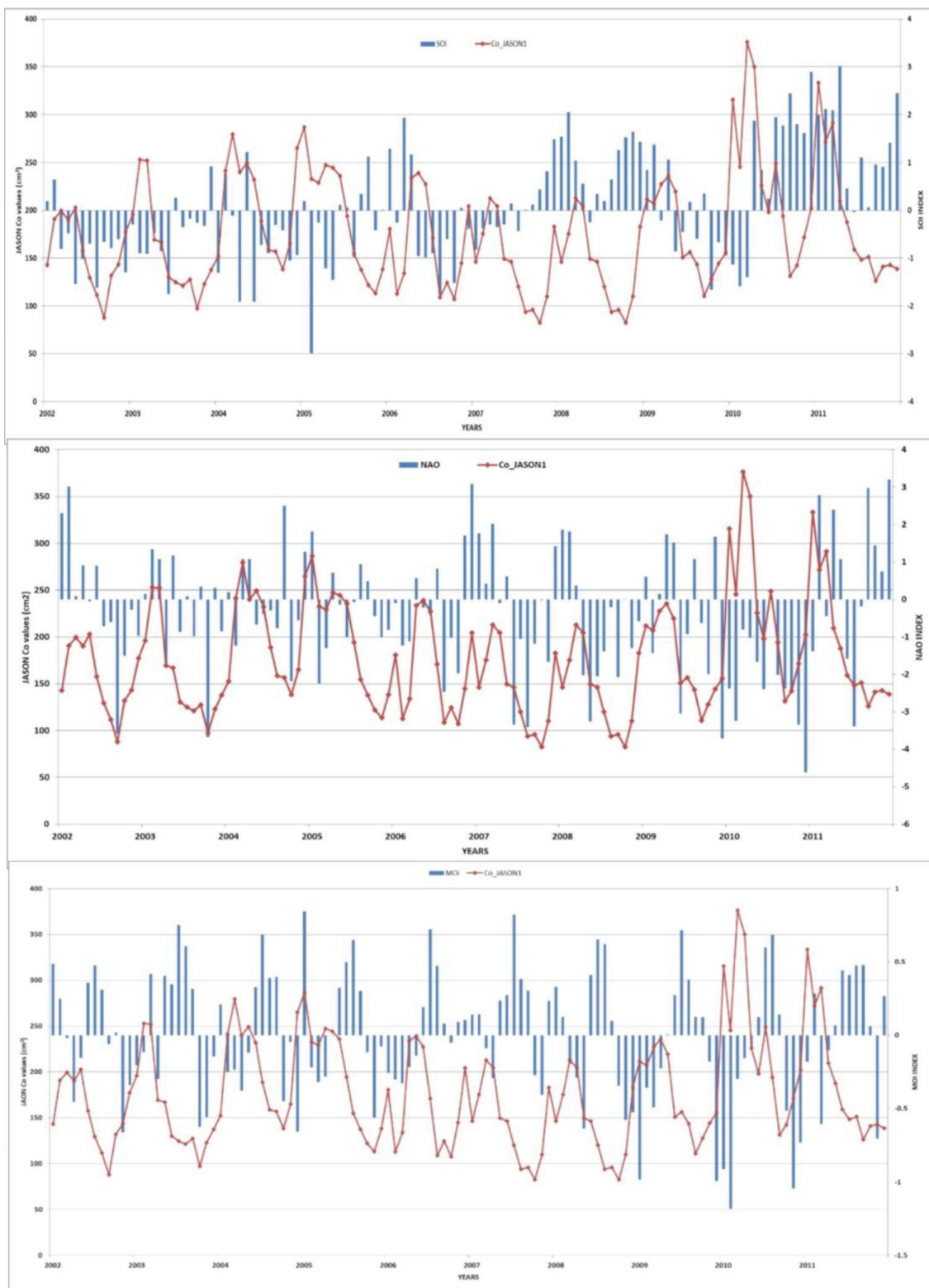
Figure 7.
Jason-1 SLA variances fluctuations from 2002 to 2011 and correlation with SOI (up), NAO (middle) and MOI (bottom).

To assess that, the MOI index has been investigated as well, since it should be the most proper measure of atmospheric forcing contribution to sea level variations in the Mediterranean. As it is clearly depicted in the bottom of all figures above where the SLA variances fluctuations and correlation with MOI is studied, this index is

Figure 8.
Jason-2 SLA variances fluctuations from 2008 to 2017 and correlation with SOI (up), NAO (middle) and MOI (bottom).

strongly correlated with SLA values. Consecutive large values of MOI indicate high temperatures and decrease of SLA variances while negative values of the index are connected with SLA rise. These findings are noticed in all missions, for the first case i.e. summer 2004 for Envisat (from 247 cm^2 to 153 cm^2) and Jason-1 (from 192 cm^2 to 114 cm^2), summer 2011 and 2012 for Jason-2 (~110 cm^2 and ~ 80 cm^2) and Cryosat-2

Figure 9.
Cryosat-2 SLA variances fluctuations from 2008 to 2017 and correlation with SOI (up), NAO (middle) and MOI (bottom).

(~120 cm^2 and ~ 110 cm^2) or for negative values in early 2009 (from 138 cm^2 to 243 cm^2), 2010 (from 152 cm^2 to 334 cm^2) for Jason-2 and in late 2012 and early 2013 for Cryosat-2 when the variance increased from 182 cm^2 to 321 cm^2. However, there are some incidents that SLA fluctuations are not connected with MOI variances

13

indicating a stronger correlation with NAO for the same period, signing that currents in Atlantic are also connected with variances in sea level of Mediterranean.

3.1 EOF analysis

EOF analysis is a very used technique in geophysical sciences in order to study any possible spatial modes of variability and how they change with time. Monthly gridded values of SLAs have been used to estimate the principal components of the time series. SLA values have been gridded to a 5 arcmin step and 172 consecutive monthly data were available from September 2002 to December 2016. Note that whenever multi-mission data have been available for a specific month, then the grid generated employs all available information.

The increasing trend that is noticed worldwide ~2 mm/year [18, 57] is also depicted in the Mediterranean (see **Figure 10**) in smaller or larger scales varying through the time or the region under study. Positive trends of 0.3 ± 0.4 mm/year in the Western part and 1.3 ± 0.4 mm/year in the Eastern part [19], 4.54 ± 0.3 mm/year for the coastal areas and 4.28 ± 0.3 mm/year for the open sea were found using altimetry from TOPEX/Poseidon and tides-gauge data [58] and 2.44 ± 0.5 mm/year with similar data spanning 20 years [59]. As it also depicted in **Figure 10**, the sea level trend differs but gradually increases from the Western to the Eastern part. More significant negative trends can be noticed in the Alboran Sea between Spain and Marocco (the lowest ~ − 10 mm/year) and northern to Egypt while the largest
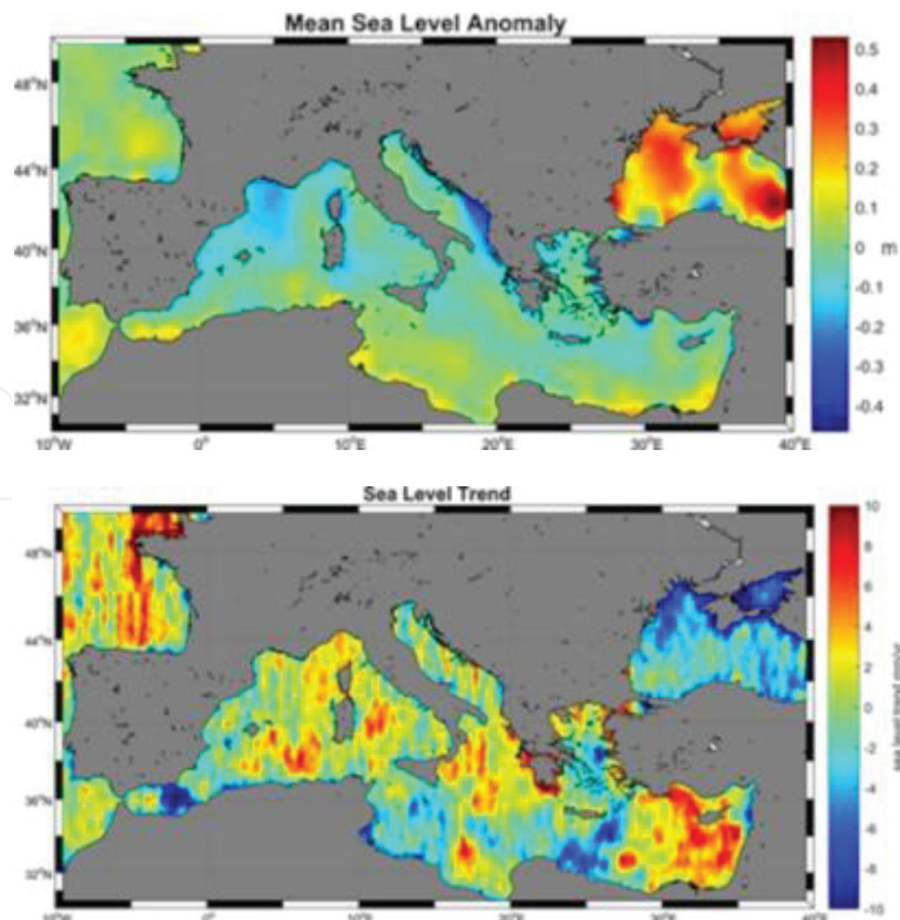
Figure 10.
*Mean SLA (m) (left) and sea level trend (right) (mm/y).*

positive trends are noticed in areas close to Peloponnese and the Levantine Sea (up to 10 cm/year). All aforementioned areas are connected with strong gyres that affect the sea level (Shikmona Gyre and Asia Minor Current in Levantine Sea, Western and Eastern Alboran Gyre in Alboran Sea) [59–64]. Similar findings are connected with the negative trends in the Ionian Sea [63, 65] and in the North Eastern part of Crete island (Ierapetra Gyre) [66, 67].

Figure 11 depicts the first EOF and first PC before removing the seasonal variability. From this Figure the annual and seasonal pattern in the SLAs are evident with the largest values occurring during the summer months and the smallest ones in the Fall. Moreover, the dominant increasing trend in the SLA is clearly depicted. After removing the trend and the seasonal signal, the EOF analysis was applied to the SLA time series for all data, in order to extract individual dominant modes of the data variability. The monthly SLA field is separated into spatial structures, the empirical orthogonal functions (EOF) and their amplitudes in time, the principle components, which are depicted in **Figure 12**. The annual signal, being 51.2% of the total variability, presents the increase of sea level that is dominant in the whole area. Modes 3 to 6,
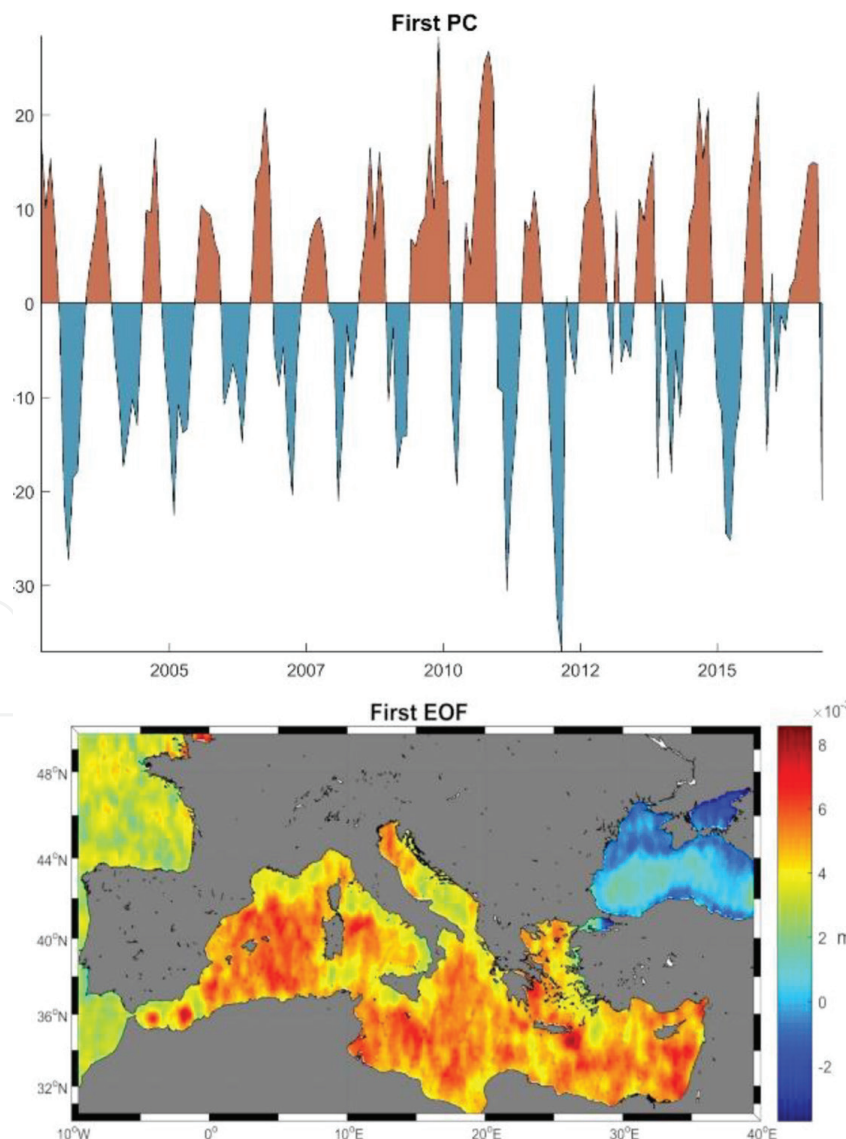
Figure 11.
First PC of SLA and first EOF before removing seasonal variability.
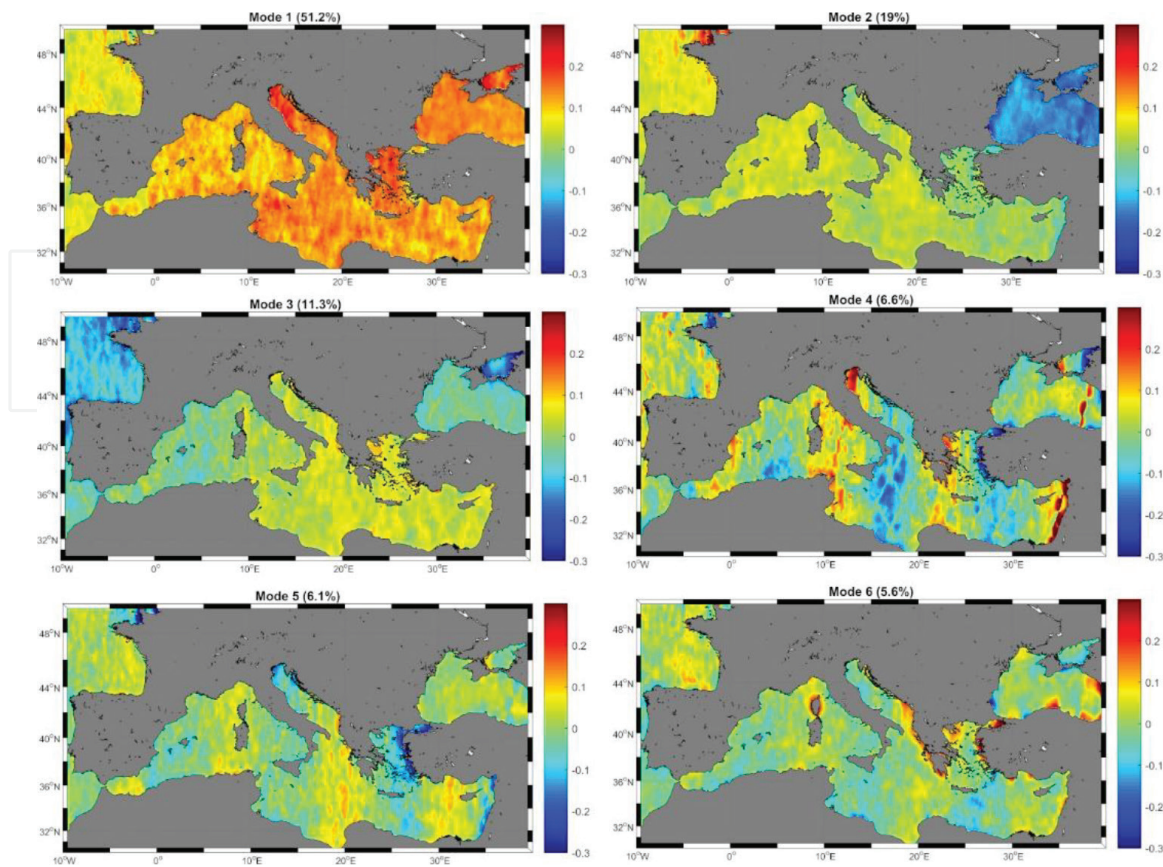
Figure 12.
First six EOF after removing seasonal variability (m).

despite having smaller percentages clearly depict local trends that can be attributed to various characteristics (different values of atmospheric pressure, entrance of ocean water from Atlantic Ocean, lake and river water that change salinity, etc.).

4. Conclusions

An analytical outline of the use of satellite altimetry data from the exact repeat missions of Envisat, Jason-1, Jason-2, and Cryosat-2 to monitor SLA variations has been presented. Through the empirical covariance functions of SLAs, it was found an important annual variation which is obvious for the whole period. This annual change follows the temperature. As the temperature rise, the water gets warmer and expands while the sea contracts when temperature decreases. This cyclo-stationary is further connected to changes in pressure in the sea level as it was clearly depicted in this work.

When the fluctuation of sea level is compared to meteorological phenomena, the El Niño and La Niña result in a slower change in the Mediterranean depending on the intensity of the events. NAO index is stronger connected to SLA variations during the late and early months of the year while MOI, as it refers to variations in pressure in Mediterranean is the most proper measure of atmospheric forcing contribution to sea level variations. Consecutive large values are connected with SLA rise while negative phases indicate decrease in variances of SLA. Finally, when the NAO and MOI are examined together, a correlation exists mainly during the cold months however this finding is not observed during the warm months indicating that circulation in Atlantic little affects the sea level in the Mediterranean.

In the last step in this work, the method of Principal Component Analysis (PCA) was applied to the SLA time series in order to extract individual dominant modes of the data variability. The dominant first PC with 51.2% presents the increase of sea level that is dominant in the whole area. Modes 3 to 6, despite having smaller percentages depict clearly local trends in the sea level in the Mediterranean.

Author details

Dimitrios A. Natsiopoulos[1], Eleni A. Tzanou[2] and Georgios S. Vergos[1]*

1 Laboratory of Gravity Field Research and Applications (GravLab), Department of Geodesy and Surveying, Aristotle University of Thessaloniki, Greece

2 Department of Surveying and Geoinformatics Engineering, International Hellenic University (IHU), Greece

*Address all correspondence to: vergos@topo.auth.gr

IntechOpen

References

[1] Fenoglio-Marc L, Tel E. Coastal and global sea level change. Journal of Geodynamics. 2010;**49**(3-4):151-160

[2] Tsimplis MN, Shaw AGP, Pascual A, Marcos M, Pasaric M, Fenoglio-Marc L. Can we reconstruct the 20th century sea level variability in the mediterranean sea on the basis of recent altimetric measurements? In: Remote Sensing of the European Seas. Netherlands: Springer; 2008. pp. 307-318

[3] Gomis D, Tsimplis M, Marcos M, Fenoglio-Marc L, Pérez B, Raicich F, et al. Mediterranean Sea-level variability and trends. In: The Climate of the Mediterranean Region. Cambridge, UK, and New York NY, USA: Cambridge University Press; 2012. pp. 257-299

[4] Weisse R, Bellafiore D, Menéndez M, Méndez F, Nicholls RJ, Umgiesser G, et al. Changing extreme sea levels along European coasts. Coastal Engineering. 2014;**87**:4-14

[5] Idier D, Paris F, Le CG, Boulahya F, Dumas F. Sea-level rise impacts on the tides of the European shelf. Continental Shelf Research. 2017;**137**(April):56-71. DOI: 10.1016/j.csr.2017.01.007

[6] Zerbini S, Raicich F, Prati CM, Bruni S, Del Conte S, Errico M, et al. Sea-level change in the northern Mediterranean Sea from long-period tide gauge time series. Earth-Science Reviews. 2017;**167**:72-87

[7] Ambrosetti E. Demographic Challenges in the Mediterranean. Eur Inst Mediterr, Mediterranean Yearbook 2020. Barcelona, Spain: IEMED Fundació CIDOB; 2020

[8] Andersen TJ, Svinth S, Pejrup M. Temporal variation of accumulation rates on a natural salt marsh in the 20th century - the impact of sea level rise and increased inundation frequency. Marine Geology. 2011;**279**(1-4):178-187. DOI: 10.1016/j.margeo.2010.10.025

[9] Pickering MD, Wells NC, Horsburgh KJ, Green JAM. The impact of future sea-level rise on the European shelf tides. Continental Shelf Research. 2012;**35**:1-15. DOI: 10.1016/j.csr.2011.11.011

[10] Pelling HE, Mattias Green JA, Ward SL. Modelling tides and sea-level rise: To flood or not to flood. Ocean Modelling. 2013;**63**:21-29. DOI: 10.1016/j.ocemod.2012.12.004

[11] Parker A. Comment to assessing sea level rise costs and adaptation benefits under uncertainty in Greece. Environmental Science & Policy. 2014;**38**:178-179. DOI: 10.1016/j.envsci.2013.12.003

[12] Dawson D, Shaw J, Roland GW. Sea-level rise impacts on transport infrastructure: The notorious case of the coastal railway line at Dawlish. England Journal of Transport Geography. 2016;**51**(February):97-109. DOI: 10.1016/j.jtrangeo.2015.11.009

[13] Kuhfuss L, Rey-Valette H, Sourisseau E, Heurtefeux H, Rufray X. Evaluating the impacts of sea level rise on coastal wetlands in Languedoc-Roussillon, France. Environmental Sciences Policy. 2016;**59**:26-34. DOI: 10.1016/j.envsci.2016.02.002

[14] Masciopinto C, Liso IS. Assessment of the impact of sea-level rise due to climate change on coastal groundwater discharge. Science of the Total Environment. 2016;**569-570**:672-680. DOI: 10.1016/j.scitotenv.2016.06.183

[15] Antonioli F, Anzidei M, Amorosi A, Lo Presti V, Mastronuzzi G, Deiana G, et al. Sea-level rise and potential drowning of the Italian coastal plains: Flooding risk scenarios for 2100. Quaternary Science Reviews. 2017;**158**:29-43. DOI: 10.1016/j.quascirev.2016.12.021

[16] Bergillos RJ, Rodriguez-Delgado C, Iglesias G. Wave farm impacts on coastal flooding under sea-level rise: A case study in southern Spain. Science of the Total Environment. 2019;**653**:1522-1531. DOI: 10.1016/j.scitotenv.2018.10.422

[17] Vergos GS, Natsiopoulos DA. Ocean remote sensing altimetric satellites in support of sea level anomalies and mean sea surface modeling. In: Perakis K, Moysiadis A, editors. Advances in Geosciences, 32nd European Association of Remote Sensing Laboratories (EARSeL) Symposia. 2013. pp. 398-423

[18] Miller L, Douglas BC. Mass and volume contributions to twentieth-century global sea level rise. Nature. 2004;**428**(6981):406-409

[19] Tsimplis MN, Álvarez-Fanjul E, Gomis D, Fenoglio-Marc L, Pérez B. Mediterranean Sea level trends: Atmospheric pressure and wind contribution. Geophysical Research Letters. 2005;**32**(20):1-4. DOI: 10.1029/2005GL023867

[20] Tsimplis M, Spada G, Marcos M, Flemming N. Multi-Decadal Sea level trends and land movements in the Mediterranean Sea with estimates of factors perturbing tide gauge data and cumulative uncertainties. Global and Planetary Change. 2010;**76**:63-76

[21] Mahdi H, Hebib T. Mediterranean Sea level trends from long-period tide gauge time series. Acta Oceanologica Sinica. 2020;**39**(1):157-165

[22] Vignudelli S, Cipollini P, Roblou L, Lyard F, Gasparini GP, Manzella G, et al. Improved satellite altimetry in coastal systems: Case study of the Corsica Channel (Mediterranean Sea). Geophysical Research Letters. 2005;**32**(7):1-5

[23] Criado-Aldeanueva F, Del Río VJ, García-Lafuente J. Steric and mass-induced Mediterranean Sea level trends from 14 years of altimetry data. Global Planet Change. 2008;**60**(3-4):563-575

[24] Birol F, Delebecque C. Using high sampling rate (10/20Hz) altimeter data for the observation of coastal surface currents: A case study over the northwestern Mediterranean Sea. Journal of Marine Systems. 2014;**129**:318-333

[25] Grgić M, Nerem RS, Bašić T. Absolute sea level surface modeling for the Mediterranean from satellite altimeter and tide gauge measurements. Marine Geodesy. 2017;**40**(4):239-258. DOI: 10.1080/01490419.2017.1342726

[26] Stammer D, Cazenave A. Satellite Altimetry over Oceans and Land Surfaces. Boca Raton, FL: CRC Press; 2017. pp. 1-618

[27] Knudsen P, Andersen O, Bingham R. Enhanced Mean Dynamic Topography and Ocean Circulation Estimation Using GOCE Preliminary Models. AGU Fall Meet Abstr. Noordwijk, Netherlands: European Space Agency; 2010

[28] Andersen OB. THE DTU12MDT Global Mean Dynamic Topography And Ocean Circulation Model. 2013 Available from: http://earth.esa.int/gut/ [Accesed: April 9, 2020]

[29] Arabelos D, Tziavos IN. Combination of ERS-1 and TOPEX altimetry for precise geoid and gravity recovery in the Mediterranean Sea. Geophysical Journal International. 1996;**125**(1):285-302

[30] Vergos GS, Tziavos IN, Andritsanos VD. On the determination of marine geoid models by least-squares collocation and spectral methods using heterogeneous data. International Association of Geodesy Symposium. 2005;**128**:332-337

[31] Tziavos IN, Vergos GS, Kotzev V, Pashova L. Mean sea level and sea level variation studies in the black sea and the Aegean. International Association of Geodesy Symposium. 2005;**129**:254-259

[32] Vergos GS, Tziavos IN, Andritsanos VD. Gravity data base generation and geoid iviodel estimation using heterogeneous data. International Association of Geodesy Symposium. 2005;**129**:155-160

[33] Cazenave A, Nerem RS. Present-Day Sea level change: Observations and causes. Reviews of Geophysics. 2004;**42**(3):1-20

[34] Church JA, White NJ, Konikow LF, Domingues CM, Cogley JG, Rignot E, et al. Revisiting the Earth's sea-level and energy budgets from 1961 to 2008. Geophysical Research Letters. 2011;**38**(18):n/a-n/a. DOI: 10.1029/2011GL048794

[35] Nerem RS, Leuliette É, Cazenave A. Present-Day Sea-level change: A review. Comptes Rendus - Geoscience. 2006;**338**(14-15):1077-1083

[36] Fernandes MJ, Barbosa S, Lázaro C. Impact of altimeter data processing on sea level studies. Sensors. 2006;**6**(3):131-163

[37] Pavlis NK, Holmes SA, Kenyon SC, Factor JK. The development and evaluation of the earth gravitational model 2008 (EGM2008). Journal of Geophysical Research. 2012;**117**:B04406. DOI: 10.1029/2011JB008916

[38] Heiskanen M. Physical Geodesy. W. A. Heiskanen and H. Moritz. pp. ix + 364, and numerous diagrams. W. H. Freeman and Co., San Francisco and London, Price 100 s. Geol Mag. 1967;**104**(3):302

[39] Allan RJ, Nicholls N, Jones PD, Butterworth IJ. A further extension of the Tahiti-Darwin SOI, early ENSO events and Darwin pressure. Journal of Climate. 1991;**4**:743-749

[40] Können G, Jones P, Kaltofen M, Allan R. Pre1866 extensions of the southern oscillation index using early Indonesian and Tahitian meteorological readings. Journal of Climate. 1998;**11**:2325-2339

[41] Ropelewski CF, Jones PD. An extension of the Tahiti–Darwin southern oscillation index. Monthly Weather Review. 1987. doi;**115**:2161-2165. DOI: 101175/1520-0493(1987)115<2161: AEOTTS>20CO;2

[42] Tsimplis MN, Josey SA. Forcing of the Mediterranean Sea by atmospheric oscillations over the North Atlantic. Geophysical Research Letters. 2001;**28**(5):803-806

[43] Osborn TJ. Recent variations in the winter North Atlantic oscillation. Weather. 2006;**61**(12):353-355. DOI: 10.1256/wea.190.06

[44] Osborn TJ. Winter 2009/2010 temperatures and a record-breaking North Atlantic oscillation index. Weather. 2011;**66**(1):19-21. DOI: 10.1002/wea.660

[45] Wakelin SL, Woodworth PL, Flather RA, Williams JA. Sea-level dependence on the NAO over the NW European continental shelf. Geophysical Research Letters. 2003;**30**(7):1403. DOI: 10.1029/2003GL017041

[46] Woolf DK, Shaw AGP, Tsimplis MN. The influence of the North Atlantic oscillation on sea-level variability in the North Atlantic region. The Global Atmosphere and Ocean System. 2003;**9**(4):145-167

[47] Palutikof J. Analysis of Mediterranean climate data: Measured and modelled. In: Mediterranean Climate. Berlin Heidelberg: Springer; 2003. pp. 125-132

[48] Tsimplis MN, Shaw AGP. The forcing of mean sea level variability around Europe. Global Planet Change. 2008;**63**(2-3):196-202

[49] Supić N, Grbec B, Vilibić I, Ivančić I. Long-term changes in hydrographic conditions in northern Adriatic and its relationship to hydrological and atmospheric processes. Annales de Geophysique. 2004;**22**(3):733-745

[50] Sušelj K, Bergant K. Mediterranean Oscillation Index. Vol. 8. Geophysical Research Abstracts; 2006. p. 02145. SRef-ID: 1607-7962/gra/EGU06-A-02145

[51] Brönnimann S. Impact of El Niño-southern oscillation on European climate. Reviews of Geophysics. 2007;**45**:RG3003. DOI: 10.1029/2006RG000199

[52] Huang B, Thorne PW, Banzon VF, Boyer T, Chepurin G, Lawrimore JH, et al. Extended reconstructed sea surface temperature, version 5 (ERSSTv5): Upgrades, validations, and intercomparisons. Journal of Climate. 2017;**30**(20):8179-8205

[53] Zhang RH, Zheng F, Zhu J, Wang Z. A successful real-time forecast of the 2010-11 la Niña event. Scientific Reports. 2013;**3**(1):1-7

[54] Paek H, Yu JY, Qian C. Why were the 2015/2016 and 1997/1998 extreme El Niños different? Geophysical Research Letters. 2017;**44**(4):1848-1856

[55] Josey SA, Somot S, Tsimplis M. Impacts of atmospheric modes of variability on Mediterranean Sea surface heat exchange. Journal of Geophys Research and Ocean. 2011;**116**(2):C02032. DOI: 10.1029/2010JC006685

[56] Tsimplis MN, Calafat FM, Marcos M, Jordà G, Gomis D, Fenoglio-Marc L, et al. The effect of the NAO on sea level and on mass changes in the Mediterranean Sea. Journal of Geophys Research and Ocean. 2013;**118**(2):944-952. DOI: 10.1002/jgrc.20078

[57] Wöppelmann G, Letetrel C, Santamaria A, Bouin MN, Collilieux X, Altamimi Z, et al. Rates of sea-level change over the past century in a geocentric reference frame. Geophysical Research Letters. 2009;**36**(12):1-6

[58] Mangiarotti S. Coastal Sea level trends from TOPEX-Poseidon satellite altimetry and tide gauge data in the Mediterranean Sea during the 1990s. Geophysical Journal International. 2007;**170**(1):132-144. DOI: 10.1111/j.1365-246X.2007.03424.x

[59] Bonaduce A, Pinardi N, Oddo P, Spada G, Larnicol G. Sea-level variability in the Mediterranean Sea from altimetry and tide gauges. Climate Dynamics. 2016;**47**:2851-2866

[60] Stanev EV, Le Traon PY, Peneva EL. Sea level variations and their dependency on meteorological and hydrological forcing: Analysis of altimeter and surface data for the black sea. Journal of Geophys Research and Ocean. 2000;**105**(C7):17203-17216

[61] Rio MH, Pascual A, Poulain PM, Menna M, Barceló B, Tintoré J. Computation of a new mean dynamic

topography for the Mediterranean Sea from model outputs, altimeter measurements and oceanographic in situ data. Ocean Science. 2014;**10**(4):731-744

[62] Rio MH, Poulain PM, Pascual A, Mauri E, Larnicol G, Santoleri R. A mean dynamic topography of the Mediterranean Sea computed from altimetric data, in-situ measurements and a general circulation model. Journal of Marine Systems. 2007;**65**(1-4 SPEC. ISS):484-508

[63] Pinardi N, Zavatarelli M, Adani M, Coppini G, Fratianni C, Oddo P, et al. Mediterranean Sea large-scale low-frequency ocean variability and water mass formation rates from 1987 to 2007: A retrospective analysis. Progress in Oceanography. 2015;**132**:318-332. DOI: 10.1016/j.pocean.2013.11.003

[64] Mohamed B, Abdallah AM, Alam El-Din K, Nagy H, Shaltout M. Inter-annual variability and trends of sea level and sea surface temperature in the Mediterranean Sea over the last 25 years. Pure and Applied Geophysics. 2019;**176**(8):3787-3810

[65] Gačić M, Civitarese G, Eusebi Borzelli GL, Kovačević V, Poulain PM, Theocharis A, et al. On the relationship between the decadal oscillations of the northern Ionian Sea and the salinity distributions in the eastern Mediterranean. Journal of Geophysical Research. 2011;**116**(C12):C12002. DOI: 10.1029/2011JC007280

[66] Fusco G, Manzella GMR, Cruzado A, Gacic M, Gasparini GP, Kovacevic V, et al. Variability of mesoscale features in the Mediterranean Sea from XBT data analysis to cite this version: Variability of mesoscale features in the Mediterranean Sea from XBT data analysis. Annales de Geophysique. 2003;**21**:21-32

[67] Marullo S, Napolitano E, Santoleri R, Manca B, Evans R. Variability of Rhodes and Ierapetra gyres during Levantine intermediate water experiment: Observations and model results. Journal of Geophys Research. 2003;**108**(C9):8119. DOI: 10.1029/2002JC001393